

Delving into 3D Action Anticipation from Streaming Videos

Hongsong Wang Jiashi Feng

Department of Electrical and Computer Engineering,
National University of Singapore

hongsongsui@gmail.com, elefjia@nus.edu.sg

Abstract

Action anticipation, which aims to recognize the action with a partial observation, becomes increasingly popular due to a wide range of applications. In this paper, we investigate the problem of 3D action anticipation from streaming videos with the target of understanding best practices for solving this problem. We first introduce several complementary evaluation metrics and present a basic model based on frame-wise action classification. To achieve better performance, we then investigate two important factors, i.e., the length of the training clip and clip sampling method. We also explore multi-task learning strategies by incorporating auxiliary information from two aspects: the full action representation and the class-agnostic action label. Our comprehensive experiments uncover the best practices for 3D action anticipation, and accordingly we propose a novel method with a multi-task loss. The proposed method considerably outperforms the recent methods and exhibits the state-of-the-art performance on standard benchmarks.

1. Introduction

Action recognition is an active research area and has witnessed great interests in the past decades. It aims to recognize an action from a video which contains a complete action execution. Many previous works focus on recognizing actions in trimmed videos each of which contains only one action instance [32, 42, 3, 39, 29]. Some other recent works can recognize actions as well as detect their starting and ending frames from untrimmed videos [46, 49, 24], where each long video contains multiple different action instances. However, these approaches mostly work in an offline fashion.

Differently, action anticipation aims to infer an action when only an early fraction of this video is observed. Action anticipation approaches [6, 16], which work in an online fashion, align better with realistic scenarios. With the increasing popularity of 3D action recognition [7, 35, 37, 40, 38], in this paper, we investigate the problem of 3D

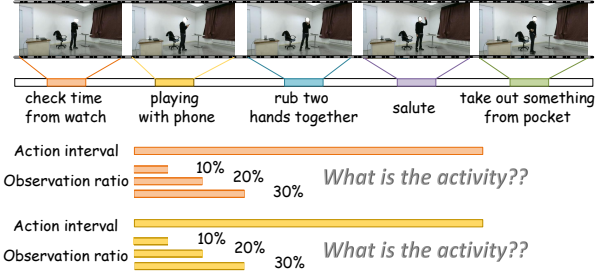


Figure 1. Illustration of action anticipation from streaming video. Given a long video containing multiple action instances, we aim to predict an action after observing only an early fraction of this instance, with 3D human skeletons. But for better visualization, we use RGB videos instead of 3D skeletons in this example.

action anticipation from streaming videos. See Figure 1 for illustration. Due to the rapid development of 3D sensors (e.g., Kinect and Asus Xtion Pro), 3D action anticipation would gain more practical applications in security surveillance, human-machine interaction, autonomous vehicles, etc.

3D action anticipation differs from traditional action recognition in several aspects. First, the input for 3D action anticipation contains no RGB videos and the recognition system relies on 3D human skeletons. Second, prediction needs to be made before the action is fully executed in an online fashion, as illustrated in Figure 1. Third, the long input video contains multiple actions as well as a large number of non-action frames.

These intrinsic characteristics raise multiple challenging questions. One is how to obtain a good basic model for 3D action anticipation from streaming videos. To this end, some good practices need be exploited. For example, since the model tends to be overwhelmed by the negative samples, how to guide the model to learn to focus on the actions instead of the background is a problem worth studying.

Another question is that whether some auxiliary information could help action anticipation. As humans are able to imagine future motions after observing some early patterns of actions, it is desirable to obtain a network to model such ability by leveraging future representation through

properly training. Moreover, as partial observations contain limited information, how to exploit other auxiliary information (e.g., class-agnostic action label) to maximally benefit action anticipation is worth investigating.

To address the above issues, we formulate the problem of 3D action anticipation from streaming videos as frame-wise 3D action recognition. We first introduce several complementary evaluation metrics. To make the performance evaluation systematic, both the anticipation accuracy and the averaged frame-wise accuracy are employed. Then, we present a basic model built on recurrent neural networks (RNN) inspired by 3D action recognition. To learn temporal dynamics of actions and achieve good generalization capability, we study the proper length of training clips. To avoid dominance of background samples and facilitate training, we propose a novel action-centric sampling scheme and also investigate the size of context window. Moreover, we explore multi-task learning strategies by incorporating some auxiliary information. To reduce the divergence between the partial action representation and the full action representation, we train a teacher network to obtain the full action representation and introduce a regression loss to minimize this divergence. We also introduce the concept of temporal actionness to utilize the class-agnostic action information and define a binary loss to discriminate between the actions and the background. Finally, we combine experimental discoveries and propose a novel loss of three terms, i.e., the frame-wise action classification loss, the full representation regression loss and the temporal actionness loss, to achieve all the benefits.

Our findings, derived from a large set of experiments, can be summarized as follows: (1) For 3D action anticipation, the length of the training clip should be relatively short. A very short clip length improves the anticipation accuracies only at the early stage, and a very long clip length even decreases the anticipation accuracies. (2) The proposed action-centric sampling scheme significantly outperforms the sliding window technique in terms of both anticipation accuracies and frame-wise accuracies. (3) Joint learning of action anticipation and full action representation improves the performance when a small proportion of an action is observed. (4) Joint learning of action anticipation and temporal actionness could better distinguish the actions from the background in the frames near the temporal boundaries of an action. (5) The effects of full action representation and temporal actionness are complementary, and state-of-the-art performance could be achieved by combining the two auxiliary information.

The remainder of the paper is organized as follows. Section 2 reviews related work. Section 3 formulates the problem and evaluation metrics. Section 4 presents the basic model and some experimental evaluations. Models using auxiliary information and related experiments are described

in Section 5. The conclusions are drawn in Section 6.

2. Related Work

In this section, we briefly review some action recognition approaches closely related to ours from two aspects, i.e., 3D action recognition and action anticipation.

3D Action Recognition. 3D human action recognition becomes popular owing to the rapid development of inexpensive depth sensors such as Kinect. We refer the reader to the recent survey papers [25, 47]. Traditional approaches mainly focus on handcrafted features, which are divided into three categories: joint based descriptors, mined joint based descriptors and dynamics based descriptors [25]. These approaches are not generic and handcrafted descriptors are not optimal for large-scale recognition.

With the surge of deep learning, recurrent neural networks (RNN) are utilized to directly learn representations from raw skeletons [34, 35, 19, 37, 40, 38, 45, 14, 15, 31]. For example, Du et al. [8, 7] designed an end-to-end hierarchical RNN architecture to hierarchically fuse the representations learned from body parts. Wang et al. [37] presented a two-stream RNN to leverage both temporal dynamics and spatial configurations of joints. Liu et al. [21, 20] presented a global context-aware attention LSTM unit to selectively focus on informative joints. Zhang et al. [48] designed a view adaptive RNN which could automatically adapt to the most suitable observation viewpoints. There are also some convolutional neural networks (CNN) based approaches [22, 10, 43]. These researches are only emphasized on action classification in manually trimmed videos.

Recently, several works focus on 3D action detection from untrimmed long videos. Li et al. [16] jointly performed frame-wise action classification and regression of the starting and ending points with an RNN structure. To facilitate large-scale 3D action detection, Liu et al. [17] collected a new benchmark named PKU-MMD and evaluated several action detection methods. Unlike these approaches, we focus on action anticipation which predicts actions from the streaming video with only early partial observations. The recent work [18] also performed online 3D action prediction, but it applied a sophisticated method and failed to study important characteristics and factors of this problem.

Action Anticipation. RGB video based action anticipation aims to predict human actions from temporally incomplete video data, and many previous works focus on trimmed short videos [27, 2, 13, 12]. For example, Ryoo et al. [27] developed a dynamic bag-of-words to model how feature distributions change over time. Lan et al. [13] developed a max-margin learning framework to describe human movements with a coarse-to-fine hierarchical representation. Kong et al. [12] proposed a multiple temporal scale support vector machine to consider both local and global temporal dynamics of actions.

Deep learning methods have also been applied for action anticipation. Ma et al. [23] introduced a new ranking loss for the predictions of LSTM to enforce that either detection score of the correct activity category or the detection score margin between the correct and incorrect categories should be monotonically non-decreasing. Aliakbarian et al. [1] introduced a novel loss function to encourage the network to predict the correct class as early as possible. Kong et al. [11] integrated LSTM with a memory module to record the discriminative information at early stage.

There are some works that aim to anticipate actions from untrimmed streaming videos. De Geest et al. [6] introduced a realistic dataset composed of TV series to encourage the research of online action detection. Gao et al. [9] learned to anticipate a sequence of future representations based on multiple history representations. These approaches mainly depend on appearance information from RGB videos. The problem of 3D action anticipation by using motion information from human skeletons has been less investigated.

3. 3D Action Anticipation

In this section, we first introduce the problem 3D action anticipation from streaming videos, then describe two complementary evaluation metrics and the primary dataset.

3.1. Problem Statement

For 3D action anticipation, the input is an untrimmed sequence of 3D human skeletons. There is a wide variety of irrelevant negative data in the long sequence. The actions in the sequence need to be detected as early as possible only with partial observations.

Let $X = [x_1, \dots, x_k, \dots, x_T]$ be the untrimmed video, where x_k is the input of the k -th frame and T is the number of frames, and X has multiple action instances. We assume that two intervals of action instances in the long sequence have no overlap, i.e., one frame can only be annotated with an action at most. An action instance is denoted by (s_i, e_i, a_i) , where s_i, e_i index the starting and ending frames and a_i is the action class. Many previous action detection approaches such as [38, 49] predict action classes as well as starting and ending frames after the whole sequence is observed. These approaches are named offline action detection. In contrast, online action detection is to detect the action in the video stream as soon as it happens. The detection only depends on past and current frames but not future frames. 3D action anticipation belongs to online action detection. For simplicity, let $[a, b]$ be the intervals from the a -th frame to the b -th frame. The aim of this task is to predict the action class a_i with a partial observation of the interval $[s_i, e_i]$ after the action starts and before the action ends.

As the sequence contains frames without any meaningful actions, we augment the action classes with a background class to annotate these frames. Online frame-wise predic-

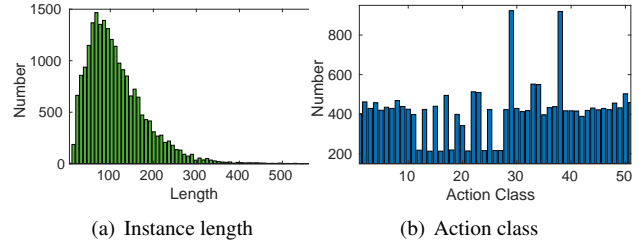


Figure 2. Number of action instance of the PKU-MMD [17] dataset. (a) Number of action instance with respect to its length. (b) Number of action instance with respect to the action class.

tions of action classes are made for the observed frames from the streaming video. Let $X(1:t) = [x_1, x_2, \dots, x_t]$ and $P(1:t) = [p_1, p_2, \dots, p_t]$ be the observed video and predicted action class probabilities from the first frame to the current t -th frame, respectively. The dimension of p_t equals to the number of the augmented classes. We aim to develop a model which outputs $P(1:t)$ based on the input of $X(1:t)$, i.e., $P(1:t) = f(X(1:t))$, where f denotes the sequence model.

3.2. Evaluation Metric

To evaluate the results of 3D action anticipation from streaming videos, we consider metrics from two aspects: anticipation accuracy of action instance and averaged frame-wise accuracy over classes. Previous works of action anticipation only use the first metric [11, 1].

To describe anticipation accuracy from the streaming video, we first define an observation ratio γ ($0 \leq \gamma \leq 1$) as the proportion of the number of frames partially observed in an action instance. After the action instance (s_i, e_i, a_i) starts in the video, the observation ratio for the t -th frame is $\frac{t-s_i}{\tau_i}$, where $\tau_i = e_i - s_i$ is the length of the action instance, and $s_i \leq t \leq e_i$. The lengths are varied for both different videos and different action instances. Then we uniformly divide the action interval $[s_i, e_i]$ of an action instance into M segments, and use the interval $[s_i + \tau_i \cdot \frac{k-1}{M}, s_i + \tau_i \cdot \frac{k}{M}]$ to denote the k -th segment, where $k \in \{1, 2, \dots, M\}$. For the sake of simplicity, the observation ratio takes values from a fixed set, i.e., $\gamma \in \{\frac{1}{M}, \dots, \frac{k}{M}, \dots, \frac{M-1}{M}\}$. When the observation ratio $\gamma = \frac{k}{M}$, the observed interval of the action instance (s_i, e_i, a_i) is $[s_i, s_i + \tau_i \cdot \frac{k}{M}]$ and the observed interval of the sequence is $[1, s_i + \tau_i \cdot \frac{k}{M}]$. For each value of the observation ratio, we predict the action label in the observed interval of the action instance based on the observed interval of the sequence. We measure the averaged predicted accuracy of all action instances for the testing set, and regard it as anticipation accuracy (Anticipation Acc).

The anticipation accuracy only considers action instances in the untrimmed video, and neglect frames without actions. The model with high anticipation accuracies are likely to wrongly recognize the frames of the background

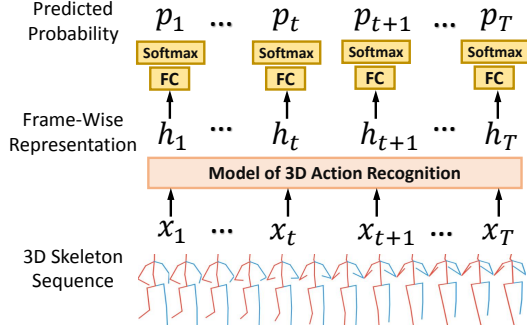


Figure 3. A basic model for 3D action anticipation.

class as a particular action. To remedy this problem, we use frame-wise accuracy to evaluate how many frames are correctly labeled after the untrimmed video has been fully observed. We report the averaged frame-wise accuracy of all categories (Avg Acc w/ bg). As the frames in a video can be dominated by the background class, the model could achieve high frame-wise accuracy by simply classifying all the frames as that class. Consequently, we also use the metric of the averaged frame-wise accuracy without background (Avg Acc w/o bg) to compute the frame-wise accuracy for the frames except the background frames.

3.3. Dataset

Most 3D action recognition datasets are intended for action classification from trimmed videos. There are a few datasets collected for temporal action detection from long untrimmed videos. PKU-MMD [17] is a recent large-scale dataset captured by the Kinect v2 sensor. It contains color images, depth images, infrared sequences and human skeletons. The dataset has 1000 long sequences with a total number of 5,312,580 frames, and more than 20,000 action instances. Each sequence contains 20 action instances, lasting about 54 minutes with a frame rate of 30 FPS. The sequences are recorded by 66 distinct subjects, whose ages range from 18 to 40. There are 43 daily actions and 8 interaction actions. The numbers of instances with respect to its length and the action class are depicted in Figure 2. Unless otherwise specified, we use the cross-subject evaluation [17] for a variety of experimental studies, and do not evaluate on other small-scale and less popular datasets.

4. Good Practices

We first present a basic model for 3D action anticipation, and then investigate two important factors to achieve good performance. Experimental evaluations of these factors are performed and some conclusions are reached.

4.1. A Basic Model

Similar to some approaches of temporal action detection [33, 38], we cast the problem as frame-wise 3D action classification based on the first observed t -th frames from

the long sequence. As depicted in Figure 3, some 3D action recognition models can be used as the backbone to learn frame-wise representations from human skeletons. Without loss of generality, we consider three layers of RNN with LSTM as the basic unit. It has been shown that this RNN structure could yield good performance for 3D action recognition [38, 48]. After learning frame-wise representations, a fully connected layer with softmax activation is used to predict class probabilities. During training, the loss L_c is:

$$L_c = -\frac{1}{T} \sum_{t=1}^T \log(p_t(y_t)) \quad (1)$$

where y_t is the ground truth class label of the t -th frame, and $p_t(y_t)$ denotes the y_t component of p_t . It should be noted that other sequence models, i.e., encoder-decoder RNN [5], temporal convolutional neural networks (CNN) [26], could also be used as the backbone, and finding the optimal sequence model is beyond the scope of this paper.

4.2. Length of Training Clip

Some actions could be identified almost instantaneously by appearance information. For RGB video based action recognition, a few frames contain sufficient appearance information such as human silhouettes, body poses, objects and scenes. Experimental studies suggest that actions could be correctly identified from very short snippets of 1-7 frames at a frame rate of 25 frames per second (FPS) [28]. By contrast, 3D action recognition often makes use of motion cues from the long sequence as the input skeletons do not provide appearance information. The training sequence could be as long as 100 frames for the NTU RGB+D dataset [30] and 200 frames for the PKU-MMD dataset [17] as reported by the state-of-the-art approaches [37, 38, 48].

For 3D action anticipation, prediction is made when only a fraction of the video frames is observed in the testing phase. As the input is an long untrimmed video, the training data should be clips sampled from the raw video. If the length of training clips is long, the network is likely to overfit frames near the end of an action. The divergence between the fully observed training data and the partially observed testing data would result in decreasing generalization ability of the model. If the length of training clips is too short, the input clip may not contain enough motion information to identify the actions. The network could not converge due to the small inter-class variability and large intra-class variability. Therefore, we aim to investigate the proper length of training clips.

The clip length is selected from a set of quantized values range from 10 to 200, and the results are summarized in Table 1. It should be noted that for the PKU-MMD dataset, most action instances are between 50 and 150 frames in length, and the averaged length of all action instances is 114. See Figure 2 for details.

We find that, when the observation ratio γ is small, i.e., $\gamma \leq 0.3$, the anticipation accuracies are higher with a smaller length of training clip. But when $\gamma \geq 0.4$, the best results are achieved when the clip length is around 40. When the clip gets longer than 40, anticipation accuracies drop monotonically. When the clip length is shorter than 40, anticipation accuracies with observation ratio $\gamma \geq 0.4$ also decrease monotonically with a smaller length of training clip. It is interpreted that results of action anticipation with smaller observation ratios rely more on local motions contained in short clips than global motions contained in long clips. So, anticipation accuracies when $\gamma \leq 0.3$ could be improved with a small length of training clip. In addition, feeding relatively short clips for training improves the generalization ability of the network, as there are fewer divergences in short clips between the training data and testing data. Conversely, the network can be easily overfitted by long training clips as it tends to be overwhelmed by the frames with large observation ratios. Actually, the values of cross entropy loss after convergence are 0.151, 0.652 and 1.395 when the clip lengths are 200, 40 and 10, respectively. The small value of the clip length also results a great diversity of training clips, which makes it hard for the model to fit the training clips well enough.

In terms of frame-wise accuracy, when the clip gets longer, both Avg Acc w/ bg and Avg Acc w/o bg first increase and then decrease. The best clip lengths of both Avg Acc w/ bg and Avg Acc w/o bg are around 50. In addition, Avg Acc w/ bg is higher than Avg Acc w/o bg when the clip is long. It is interpreted that a long clip comprises a large proportion of background frames, so Avg Acc w/ bg could be enhanced. When the clip length is short, the frame-wise accuracies are relatively low due to large intra-class variability. If the clip continues to increase when it is greater than a certain value, frame-wise accuracies could be diminished due to the potential overfitting.

The results of experiments confirm our hypothesis that a relatively short training clip benefits action anticipation. To balance the anticipation accuracies and the averaged frame-wise accuracies, a good clip length is around the half of the averaged length of action instances. In the following studies, we set the clip length to 50, unless otherwise specified.

4.3. Sampling Strategy

As the input video has thousands of frames, it is unrealistic to train a model with the long sequence. In addition, most of the frames are not related to actions. The averaged video length of the PKU-MMD [17] dataset is 4854, and the number of frames of 51 actions only accounts for 47.0% of the total number of frames. One common strategy is to use the sliding window technique to generate a subset of clips of a fixed length during training. However, labels of the sampled clips can be dominated by the background class.

An effective sampling method should sample discriminative examples and obtain a proper balance in the training set between positive samples and negative samples. We proposed a novel action-centric sampling scheme. Let (s_i, e_i, a_i) be an action instance, where s_i, e_i are the starting and ending frames and a_i is the action class. We define the action-centric interval as $[s_i - w, e_i + w]$, where w is the size of the context window. This interval contains the action instance as well as the neighboring frames before the action starts and after the action ends. The neighboring frames are regarded as the context of the action, and w is a parameter to determine the number of context frames. During training, we uniformly draw clips of a fixed length from the action-centric interval. During testing, a sliding window is utilized to draw clips from the start to the end of the long sequence, and the predictions of sampled clips are concatenated to obtain frame-wise predictions. The action-centric sampling scheme does not suffer from excessive background frames without actions. Moreover, neighboring frames are negative samples which are hard to distinguish from the positive action instances.

The results are shown in Figure 4. For the sake of convenience, the action-centric sampling scheme and the sliding window technique are denoted as AC and SW, respectively. We also alternately apply the two sampling methods for different epochs during training and denote the hybrid sampling method as AC/SW. While comparing the anticipation accuracies in Figure 4(a), we find that AC significantly outperforms both SW and AC/SW under different observation ratios. For example, when the observation ratio is 0.9, the anticipation accuracy of AC is 15% higher than that of SW. Figure 4(b) illustrates the results of frame-wise accuracies. For both Avg Acc w/bg and Avg Acc w/o bg, AC yields the best performance. For example, for Avg Acc w/o bg, AC outperforms SW and AC/SW by 10.5% and 8.6%, respectively. The results demonstrate the effectiveness of the proposed action-centric sampling scheme.

We next experimentally investigate the length of the context window w . Intuitively, a small w means there are less negative frames and the model could fail to distinguish between the background class and the actions. On the other hand, a large w leads to redundancy and the training samples could also be dominated by the background class. The results are summarized in Figure 5. Generally, when the length of the context window is small (e.g., $w < 25$), anticipation accuracies increase with the increase of the context window. When the context window gets larger (e.g., $w > 30$), anticipation accuracies decrease. Excellent results can be achieved when the context window length is between 20 and 30. The best context window size is around the half of the length of the training clip. In terms of frame-wise accuracy, similar results can be observed for both Avg Acc w/ bg and Avg Acc w/o bg.

Table 1. Action anticipation results vs. the length of training clip. The observing ratio takes the value from the set $\{0.1, 0.2, \dots, 0.9\}$.

| Clip length | Anticipation Acc | | | | | | | | | Avg Acc | |
|-------------|------------------|-------|-------|-------|-------|-------|-------|-------|-------|---------|--------|
| | 0.1 | 0.2 | 0.3 | 0.4 | 0.5 | 0.6 | 0.7 | 0.8 | 0.9 | w/ bg | w/o bg |
| 10 | 0.381 | 0.549 | 0.658 | 0.713 | 0.739 | 0.759 | 0.764 | 0.769 | 0.772 | 0.582 | 0.585 |
| 20 | 0.362 | 0.531 | 0.649 | 0.706 | 0.734 | 0.752 | 0.766 | 0.776 | 0.780 | 0.607 | 0.608 |
| 40 | 0.289 | 0.497 | 0.634 | 0.720 | 0.765 | 0.790 | 0.812 | 0.822 | 0.824 | 0.646 | 0.643 |
| 50 | 0.270 | 0.488 | 0.632 | 0.712 | 0.763 | 0.790 | 0.809 | 0.815 | 0.819 | 0.651 | 0.649 |
| 80 | 0.249 | 0.446 | 0.588 | 0.675 | 0.734 | 0.767 | 0.794 | 0.803 | 0.804 | 0.651 | 0.647 |
| 100 | 0.260 | 0.442 | 0.571 | 0.656 | 0.706 | 0.740 | 0.760 | 0.771 | 0.776 | 0.642 | 0.638 |
| 160 | 0.236 | 0.404 | 0.527 | 0.609 | 0.665 | 0.703 | 0.730 | 0.747 | 0.753 | 0.632 | 0.626 |
| 200 | 0.222 | 0.398 | 0.526 | 0.617 | 0.672 | 0.707 | 0.732 | 0.750 | 0.753 | 0.636 | 0.631 |

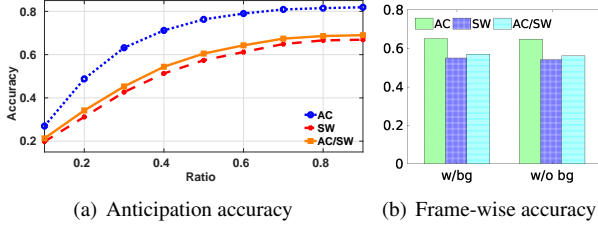


Figure 4. Action anticipation results vs. clip sampling methods. (a) Anticipation accuracies vs. the observation ratio. (b) Frame-wise accuracies (w/bg and w/o bg are short for Avg Acc w/bg and Avg Acc w/o bg, respectively).

In sum, to guide the network to learn to focus on the actions instead of the background, training clips need to be sampled around action instances. A context window is useful to include the hard negative samples and balance the number of between the positive and the negative. Note that the values of parameters depend on the choice of dataset.

5. Utilizing Auxiliary Information

Based on the basic model, we develop an improved model by incorporating some auxiliary information and provide corresponding experimental results and analysis. We further propose a novel method with a multi-task loss and compare it with the state-of-the-art approaches.

5.1. Full Action Representation

Action anticipation is challenging because predictions must be made given temporally incomplete action executions. As humans could imagine future motions after observing some particular temporal patterns of actions at the early stage, an intuitive idea is that we could predict future representation based on the incomplete action observation. There are several previous works which exploit similar intuitions. For example, Vondrick et al. [36] learned to predict the representation of future frame from the unlabeled video. Gao et al. [9] took multiple history representations as input and predict a sequence of future representations. Different from previous approaches, we first exploit this idea for 3D action anticipation by using a multi-task learning paradigm.

Let $X(1:t) = [x_1, x_2, \dots, x_t]$ denote the observed sequence, and $[s_i, e_i]$ be the interval of an action instance. To describe this model, we assume that $s_i \leq t \leq e_i$, i.e., the action instance is partially observed. The sequence model maps a sequence of input $X(1:t)$ to a sequence of output $H(1:t) = [h_1, h_2, \dots, h_t]$, where h_t is the learned representation of the t -th frame. Let the representations of the partially observed action instance be $H(s_i:t) = [h_{s_i}, \dots, h_t]$. We call the representation of the fully observed action instance as the full action representation, and denote it by h_{e_i} . To predict the future representation and reduce the divergence between h_t and h_{e_i} , a projection matrix is used to map between the two representations. The full representation regression loss L_r to be minimized is:

$$L_r = \frac{1}{e_i - s_i} \sum_{t=s_i}^{e_i} \|Wh_t - h_{e_i}\|_2^2 \quad (2)$$

where W is the projection matrix, which is jointly trained with the sequence model.

Since the ground truth of the full action representation is not available, we utilize another RNN based model with the same architecture as a side network to learn this representation. The process is illustrated in Figure 6. For each action instance, the output of the side network at the last frame is regarded as the full action representation. The two networks could be trained simultaneously by leveraging the student teacher networks [44]. As the main goal is to analyze the effects of the auxiliary full action representation, we use a simple but effective strategy. We first train the side network and use the pretrained model to predict the full action representation based on the full observation an action instance. The predicted full action representation is used as the ground truth during multi-task training. For testing, the side network is discarded and frame-wise prediction is performed for the long input sequence.

The loss of joint learning of action anticipation and full action representation is:

$$L = L_c + \alpha L_r \quad (3)$$

where α is the weight of the regression loss.

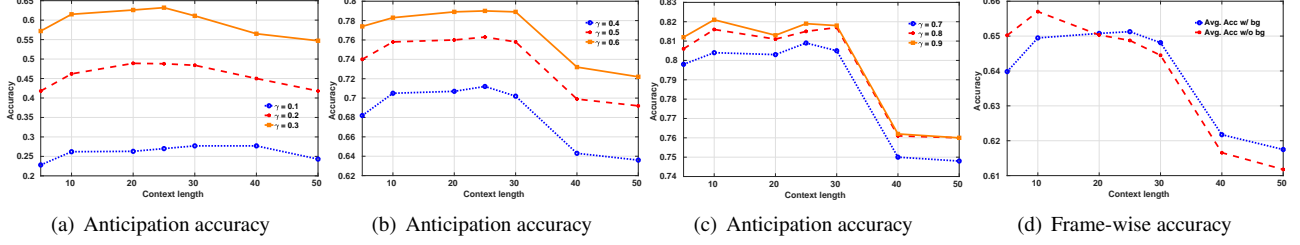


Figure 5. Action anticipation results vs. the size of the context window. The context length is selected from a set of values range from 5 to 50, and γ is the observation ratio.

Table 2. Results of joint learning of action anticipation and full action representation, and α is the weight of regression loss.

| α | Anticipation Acc | | | | | | | | | Avg Acc | |
|----------|------------------|-------|-------|-------|-------|-------|-------|-------|-------|---------|--------|
| | 0.1 | 0.2 | 0.3 | 0.4 | 0.5 | 0.6 | 0.7 | 0.8 | 0.9 | w/ bg | w/o bg |
| 0 | 0.270 | 0.488 | 0.632 | 0.712 | 0.763 | 0.790 | 0.809 | 0.815 | 0.819 | 0.651 | 0.649 |
| 0.01 | 0.319 | 0.520 | 0.639 | 0.713 | 0.760 | 0.786 | 0.809 | 0.816 | 0.822 | 0.653 | 0.650 |
| 0.1 | 0.301 | 0.517 | 0.641 | 0.722 | 0.766 | 0.789 | 0.803 | 0.811 | 0.813 | 0.657 | 0.655 |
| 1 | 0.303 | 0.507 | 0.643 | 0.722 | 0.763 | 0.792 | 0.810 | 0.821 | 0.819 | 0.657 | 0.655 |
| 10 | 0.308 | 0.527 | 0.653 | 0.730 | 0.767 | 0.794 | 0.805 | 0.820 | 0.820 | 0.660 | 0.658 |

Table 3. Results of joint learning of action anticipation and temporal actionness. Here, β is the weight of temporal actionness loss.

| β | Anticipation Acc | | | | | | | | | Avg Acc | |
|---------|------------------|-------|-------|-------|-------|-------|-------|-------|-------|---------|--------|
| | 0.1 | 0.2 | 0.3 | 0.4 | 0.5 | 0.6 | 0.7 | 0.8 | 0.9 | w/ bg | w/o bg |
| 0 | 0.270 | 0.488 | 0.632 | 0.712 | 0.763 | 0.790 | 0.809 | 0.815 | 0.819 | 0.651 | 0.649 |
| 0.1 | 0.299 | 0.517 | 0.651 | 0.727 | 0.766 | 0.790 | 0.808 | 0.821 | 0.823 | 0.660 | 0.658 |
| 0.5 | 0.307 | 0.523 | 0.647 | 0.716 | 0.764 | 0.793 | 0.809 | 0.821 | 0.823 | 0.663 | 0.661 |
| 1 | 0.304 | 0.514 | 0.642 | 0.719 | 0.762 | 0.786 | 0.806 | 0.817 | 0.825 | 0.653 | 0.652 |
| 5 | 0.309 | 0.520 | 0.658 | 0.719 | 0.766 | 0.791 | 0.807 | 0.815 | 0.821 | 0.656 | 0.654 |

The results are shown in Table 2. When $\alpha = 0$, the model degenerates to the basic model. We observe that when the observation ratio γ is small, i.e., $\gamma \leq 0.3$, the multi-task model considerably improves the anticipation accuracy. When γ gets larger, e.g., $\gamma \geq 0.5$, the improvement is limited and the multi-task model exhibits almost the same performance as that of the basic model. The results can be explained by the proposed loss in Equation (2). When γ is small, the proposed loss encourages the network to learn representations under partial observations which are similar to the full action representation. When γ goes high, the divergence between the partial action representation and the full action representation is trivial, so the proposed loss takes little effect. Similarly, the multi-task model outperforms the basic model in terms of the averaged frame-wise accuracy with or without the background. We also find that the results are relatively robust to the weight parameter.

5.2. Temporal Actionness

The term actionness [4, 41] indicates the likelihood that a specific spatial location contains a generic action instance. Actionness map has been applied for the task of spatial-temporal action detection to generate accurate action proposals. Similarly, temporal actionness [49, 50] indicates the

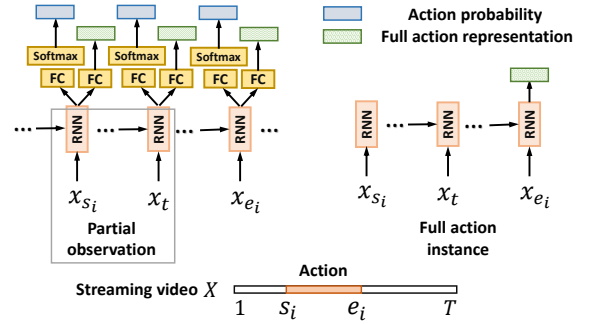


Figure 6. A framework of joint learning of action anticipation and full action representation. Here, X denotes the untrimmed video with T frames, and the interval $[s_i, e_i]$ is an action instance. We use one layer of RNN to symbolize the sequence model.

likelihood that a frame or a clip contains a generic action instance, and has proved useful for temporal action detection from untrimmed long videos. Aiming to better discriminate between the class-agnostic action and the background class, we apply temporal actionness for 3D action anticipation.

For an input video, we consider the ground truth of temporal actionness as a binary vector where 1 denotes the action classes and 0 denotes the background class. A logistic regression module is used to estimate the probability of the class-agnostic action. Specifically, a fully connected layer

Table 4. Comparison of the proposed approach with the state-of-the-art methods on the PKU-MMD dataset.

| Method | 0.1 | 0.2 | 0.3 | 0.4 | 0.5 | 0.6 | 0.7 | 0.8 | 0.9 |
|---------------|--------------|--------------|--------------|--------------|--------------|--------------|--------------|--------------|--------------|
| GCA-LSTM [21] | 0.198 | – | – | – | 0.629 | – | – | – | 0.749 |
| JCR-RNN [16] | 0.253 | – | – | – | 0.640 | – | – | – | 0.734 |
| SSNet [18] | 0.300 | – | – | – | 0.685 | – | – | – | 0.786 |
| RNN-FAC | 0.303 | 0.507 | 0.643 | 0.722 | 0.763 | 0.792 | 0.810 | 0.821 | 0.819 |
| RNN-TA | 0.304 | 0.514 | 0.642 | 0.719 | 0.762 | 0.786 | 0.806 | 0.817 | 0.825 |
| RNN-FAC-TA | 0.320 | 0.523 | 0.648 | 0.726 | 0.771 | 0.803 | 0.815 | 0.822 | 0.827 |

of 2 neurons is placed on top of the backbone. The prediction of temporal actionness is limited to a fractional value which ranges from 0 to 1. A binary cross entropy loss is applied for the frame-wise class-agnostic action classification based on partial observations. Let q_t denote the predicted temporal actionness of the t -th frame, the temporal actionness loss L_n for a sequence of T frames is:

$$L_n = -\frac{1}{T} \sum_{t=1}^T [\tilde{y}_t \log(q_t) + (1 - \tilde{y}_t) \log(1 - q_t)] \quad (4)$$

where \tilde{y}_t is the ground truth of temporal actionness.

The loss of joint learning of action anticipation and temporal actionness is:

$$L = L_c + \beta L_n \quad (5)$$

where β is the weight parameter. When $\beta = 0$, the model degenerates to basic model in Section 4.1.

Table 3 gives the experimental results. We observe that the temporal actionness term could improve the results of action anticipation, especially when the observation ratio $\gamma \in \{0.1, 0.2, 0.8, 0.9\}$. The improvements are not significant when γ takes some other values. When $\gamma \in \{0.1, 0.2, 0.8, 0.9\}$, the current observed frame is close to either the starting frame or the ending frame of an action instance. In terms of the averaged frame-wise accuracy, the multi-task model could also bring considerable improvements. The improvements are observed for a variety of values of the weight. One possible explanation is that multi-task learning with the temporal actionness could better distinguish the actions and the background class in the frames near the temporal boundaries of the action instance, thus improving the results of action anticipation.

5.3. A Multi-Task Loss

Based on the above experimental results, we propose a novel method by incorporating both the full representation regression loss and the temporal actionness loss with the frame-wise cross entropy loss. The total loss is:

$$L = L_c + \alpha L_r + \beta L_n \quad (6)$$

where α and β are the weight parameters. The details of the latter two losses are presented in Section 5.1 and 5.2.

We apply the good practices (see Section 4) for 3D action anticipation. During training, the action-centric sampling scheme is used to draw relatively small clips from the long sequence. The size of the context window is set to half the length of the training clip. For testing, frame-wise action classification is performed from beginning to end of the streaming video.

As the multi-task model is not sensitive to the values of weights, we set $\alpha = \beta = 1$ for simplicity. The proposed method is denoted as RNN-FAC-TA, and its two variants presented in Section 5.1 and 5.2 are denoted as RNN-FAC and RNN-TA, respectively. In Table 4, we compare our methods with the state-of-the-art approaches on the PKU-MMD dataset. We observe that RNN-FAC-TA outperforms both RNN-FAC and RNN-TA for all values of the observation ratio γ . Specifically, the improvements are significant when γ takes small values, i.e., $\gamma = 0.1$. The results indicate that the effects of the two proposed losses are complementary. In addition, our results are considerably higher than those of the recent approaches. When $\gamma = 0.1$ and $\gamma = 0.5$, RNN-FAC-TA outperforms the newly proposed SSNet [18] by 2.0% and 8.6%, respectively.

6. Conclusion

In this paper, we formulate the problem of 3D action anticipation from streaming videos and present a basic model based on frame-wise 3D action classification. We investigate several factors which would produce good performance. In addition, multi-task learning by some auxiliary information is also explored. Through extensive experiments, we find some best practices for 3D action anticipation from human skeletons. First, the length of the training clip should be relatively short. Second, it is better to sample clips around action instances with context frames than to sample clips randomly from the long sequence. Third, multi-task learning with the full action representation improves the performance when a small proportion of an action is observed. Fourth, multi-task learning with the class-agnostic action label could better distinguish the actions and the background in the frames near the temporal boundaries of an action. Finally, a multi-task loss with frame-wise action classification, full representation regression and frame-wise class-agnostic action classification could achieve the best results. We hope our work would provide insights into

3D action anticipation and motivate researchers in related areas to continue to explore principled approaches.

References

- [1] M. S. Aliakbarian, F. S. Saleh, M. Salzmann, B. Fernando, L. Petersson, and L. Andersson. Encouraging lstms to anticipate actions very early. In *IEEE International Conference on Computer Vision*, volume 1, 2017.
- [2] Y. Cao, D. Barrett, A. Barbu, S. Narayanaswamy, H. Yu, A. Michaux, Y. Lin, S. Dickinson, J. Mark Siskind, and S. Wang. Recognize human activities from partially observed videos. In *IEEE Conference on Computer Vision and Pattern Recognition*, pages 2658–2665, 2013.
- [3] J. Carreira and A. Zisserman. Quo vadis, action recognition? a new model and the kinetics dataset. In *Computer Vision and Pattern Recognition*, pages 4724–4733. IEEE, 2017.
- [4] W. Chen, C. Xiong, R. Xu, and J. J. Corso. Actionness ranking with lattice conditional ordinal random fields. In *IEEE Conference on Computer Vision and Pattern Recognition*, pages 748–755. IEEE, 2014.
- [5] K. Cho, B. Van Merriënboer, C. Gulcehre, D. Bahdanau, F. Bougares, H. Schwenk, and Y. Bengio. Learning phrase representations using rnn encoder-decoder for statistical machine translation. In *Empirical Methods in Natural Language Processing*, 2014.
- [6] R. De Geest, E. Gavves, A. Ghodrati, Z. Li, C. Snoek, and T. Tuytelaars. Online action detection. In *European Conference on Computer Vision*, pages 269–284. Springer, 2016.
- [7] Y. Du, Y. Fu, and L. Wang. Representation learning of temporal dynamics for skeleton-based action recognition. *IEEE Transactions on Image Processing*, 25(7):3010–3022, 2016.
- [8] Y. Du, W. Wang, and L. Wang. Hierarchical recurrent neural network for skeleton based action recognition. In *IEEE Conference on Computer Vision and Pattern Recognition*, pages 1110–1118. IEEE, 2015.
- [9] J. Gao, Z. Yang, and N. Ram. RED: Reinforced encoder-decoder networks for action anticipation. In *British Machine Vision Conference*, 2017.
- [10] Q. Ke, M. Bennamoun, S. An, F. Sohel, and F. Boussaid. A new representation of skeleton sequences for 3d action recognition. In *IEEE Conference on Computer Vision and Pattern Recognition*, pages 4570–4579. IEEE, 2017.
- [11] Y. Kong, S. Gao, B. Sun, and Y. Fu. Action prediction from videos via memorizing hard-to-predict samples. In *AAAI*, 2018.
- [12] Y. Kong, D. Kit, and Y. Fu. A discriminative model with multiple temporal scales for action prediction. In *European conference on computer vision*, pages 596–611. Springer, 2014.
- [13] T. Lan, T.-C. Chen, and S. Savarese. A hierarchical representation for future action prediction. In *European Conference on Computer Vision*, pages 689–704. Springer, 2014.
- [14] I. Lee, D. Kim, S. Kang, and S. Lee. Ensemble deep learning for skeleton-based action recognition using temporal sliding lstm networks. In *International Conference on Computer Vision*, pages 1012–1020. IEEE, 2017.
- [15] W. Li, L. Wen, M.-C. Chang, S.-N. Lim, and S. Lyu. Adaptive rnn tree for large-scale human action recognition. In *IEEE International Conference on Computer Vision*, pages 1453–1461, 2017.
- [16] Y. Li, C. Lan, J. Xing, W. Zeng, C. Yuan, and J. Liu. Online human action detection using joint classification-regression recurrent neural networks. In *European Conference on Computer Vision*, pages 203–220. Springer, 2016.
- [17] C. Liu, Y. Hu, Y. Li, S. Song, and J. Liu. PKU-MMD: A large scale benchmark for continuous multi-modal human action understanding. *arXiv preprint arXiv:1703.07475*, 2017.
- [18] J. Liu, A. Shahroudy, G. Wang, L.-Y. Duan, and A. C. Kot. SSNet: Scale selection network for online 3d action prediction. In *IEEE Conference on Computer Vision and Pattern Recognition*, pages 8349–8358. IEEE, 2018.
- [19] J. Liu, A. Shahroudy, D. Xu, and G. Wang. Spatio-temporal lstm with trust gates for 3d human action recognition. In *European Conference on Computer Vision*, pages 816–833. Springer, 2016.
- [20] J. Liu, G. Wang, L.-Y. Duan, K. Abdiyeva, and A. C. Kot. Skeleton based human action recognition with global context-aware attention lstm networks. *IEEE Transactions on Image Processing*, 27(4):1586–1599, 2017.
- [21] J. Liu, G. Wang, P. Hu, L.-Y. Duan, and A. C. Kot. Global context-aware attention lstm networks for 3d action recognition. In *IEEE Conference on Computer Vision and Pattern Recognition*, pages 3671–3680. IEEE, 2017.
- [22] M. Liu, H. Liu, and C. Chen. Enhanced skeleton visualization for view invariant human action recognition. *Pattern Recognition*, 68:346–362, 2017.
- [23] S. Ma, L. Sigal, and S. Sclaroff. Learning activity progression in lstms for activity detection and early detection. In *IEEE Conference on Computer Vision and Pattern Recognition*, pages 1942–1950. IEEE, 2016.
- [24] A. Piergiovanni and M. S. Ryoo. Learning latent super-events to detect multiple activities in videos. In *IEEE Conference on Computer Vision and Pattern Recognition*, volume 4. IEEE, 2018.
- [25] L. L. Presti and M. La Cascia. 3D skeleton-based human action classification: A survey. *Pattern Recognition*, 53:130–147, 2016.
- [26] C. L. M. D. F. René and V. A. R. G. D. Hager. Temporal convolutional networks for action segmentation and detection. In *IEEE International Conference on Computer Vision*. IEEE, 2017.
- [27] M. S. Ryoo. Human activity prediction: Early recognition of ongoing activities from streaming videos. In *IEEE International Conference on Computer Vision*, pages 1036–1043. IEEE, 2011.
- [28] K. Schindler and L. Van Gool. Action snippets: How many frames does human action recognition require? In *IEEE Conference on Computer Vision and Pattern Recognition*, pages 1–8. IEEE, 2008.
- [29] L. Sevilla-Lara, Y. Liao, F. Guney, V. Jampani, A. Geiger, and M. J. Black. On the integration of optical flow and action recognition. In *IEEE Conference on Computer Vision and Pattern Recognition*. IEEE, 2018.

- [30] A. Shahroudy, J. Liu, T.-T. Ng, and G. Wang. NTU RGB+D: A large scale dataset for 3d human activity analysis. In *IEEE Conference on Computer Vision and Pattern Recognition*, pages 1010–1019. IEEE, 2016.
- [31] C. Si, Y. Jing, W. Wang, L. Wang, and T. Tan. Skeleton-based action recognition with spatial reasoning and temporal stack learning. *arXiv preprint arXiv:1805.02335*, 2018.
- [32] K. Simonyan and A. Zisserman. Two-stream convolutional networks for action recognition in videos. In *Advances in Neural Information Processing Systems*, pages 568–576, 2014.
- [33] B. Singh, T. K. Marks, M. Jones, O. Tuzel, and M. Shao. A multi-stream bi-directional recurrent neural network for fine-grained action detection. In *IEEE Conference on Computer Vision and Pattern Recognition*, pages 1961–1970, 2016.
- [34] S. Song, C. Lan, J. Xing, W. Zeng, and J. Liu. An end-to-end spatio-temporal attention model for human action recognition from skeleton data. In *AAAI*, 2017.
- [35] S. Song, C. Lan, J. Xing, W. Zeng, and J. Liu. Spatio-temporal attention-based lstm networks for 3d action recognition and detection. *IEEE Transactions on Image Processing*, 27(7):3459–3471, 2018.
- [36] C. Vondrick, H. Pirsiavash, and A. Torralba. Anticipating visual representations from unlabeled video. In *IEEE Conference on Computer Vision and Pattern Recognition*, pages 98–106. IEEE, 2016.
- [37] H. Wang and L. Wang. Modeling temporal dynamics and spatial configurations of actions using two-stream recurrent neural networks. In *IEEE Conference on Computer Vision and Pattern Recognition*. IEEE, 2017.
- [38] H. Wang and L. Wang. Beyond joints: Learning representations from primitive geometries for skeleton-based action recognition and detection. *IEEE Transactions on Image Processing*, 27(9):4382–4394, 2018.
- [39] H. Wang and L. Wang. Cross-agent action recognition. *IEEE Transactions on Circuits and Systems for Video Technology*, 28(10):2908–2919, 2018.
- [40] H. Wang and L. Wang. Learning content and style: Joint action recognition and person identification from human skeletons. *Pattern Recognition*, 81:23–35, 2018.
- [41] L. Wang, Y. Qiao, X. Tang, and L. Van Gool. Actionness estimation using hybrid fully convolutional networks. In *IEEE Conference on Computer Vision and Pattern Recognition*, pages 2708–2717. IEEE, 2016.
- [42] L. Wang, Y. Xiong, Z. Wang, Y. Qiao, D. Lin, X. Tang, and L. Van Gool. Temporal segment networks: Towards good practices for deep action recognition. In *European Conference on Computer Vision*, pages 20–36. Springer, 2016.
- [43] P. Wang, W. Li, Z. Gao, J. Zhang, C. Tang, and P. O. Ogunbona. Action recognition from depth maps using deep convolutional neural networks. *IEEE Transactions on Human-Machine Systems*, 46(4):498–509, 2016.
- [44] J. H. Wong and M. J. Gales. Sequence student-teacher training of deep neural networks. 2016.
- [45] S. Yan, Y. Xiong, and D. Lin. Spatial temporal graph convolutional networks for skeleton-based action recognition. In *AAAI*. IEEE, 2018.
- [46] S. Yeung, O. Russakovsky, G. Mori, and L. Fei-Fei. End-to-end learning of action detection from frame glimpses in videos. In *IEEE Conference on Computer Vision and Pattern Recognition*, pages 2678–2687, 2016.
- [47] J. Zhang, W. Li, P. O. Ogunbona, P. Wang, and C. Tang. RGB-D-based action recognition datasets: A survey. *Pattern Recognition*, 60:86–105, 2016.
- [48] P. Zhang, C. Lan, J. Xing, W. Zeng, J. Xue, N. Zheng, et al. View adaptive recurrent neural networks for high performance human action recognition from skeleton data. In *International Conference on Computer Vision*. IEEE, 2017.
- [49] Y. Zhao, Y. Xiong, L. Wang, Z. Wu, X. Tang, and D. Lin. Temporal action detection with structured segment networks. *International Conference on Computer Vision*, 2, 2017.
- [50] Y. Zhu and S. Newsam. Efficient action detection in untrimmed videos via multi-task learning. In *IEEE Winter Conference on Applications of Computer Vision*, pages 197–206. IEEE, 2017.